Published in final edited form as:
Brain Res. 2013 November 6; 1537: . doi:10.1016/j.brainres.2013.08.053.

BOLD Response to Working Memory Not Related to Cortical Thickness during Early Adolescence

Lindsay M. Squeglia, Ph.D.[b,*], **Benjamin S. McKenna, Ph.D.**[a,b], **Joanna Jacobus, Ph.D.**[a,b], **Norma Castro, M.A.**[b], **Scott F. Sorg, M.S.**[c], and **Susan F. Tapert, Ph.D.**[a,b]

[a]VA San Diego Healthcare System, La Jolla, California, USA

[b]University of California San Diego, Department of Psychiatry, La Jolla, California, USA

[c]San Diego State University/University of California San Diego Joint Doctoral Program in Clinical Psychology, San Diego, California, USA

Abstract

Background—Significant cortical thinning and neural resource allocation changes emerge during adolescence; however, little is known of how morphometric changes influence neural response to cognitive demands. This study used a novel multimodal imaging registration technique to examine the relationship between brain structure and function during adolescence.

Methods—156 healthy 12–14 year-olds (44% female) participants underwent structural and functional magnetic resonance imaging. Cortical surface reconstruction was performed via FreeSurfer, and neural activation was measured from a blood oxygen level dependent (BOLD) contrast during visual working memory (VWM) via AFNI. AFNI Surface Mapper aligned segmented volumetric and functional datasets to a common template space. Hierarchical linear regressions determined the effect of cortical thickness on VWM BOLD contrast in brain regions that activated during the VWM task, controlling for age, pubertal development, gender, IQ, and intracranial volume.

Results—Power analyses suggest this study was able to detect small effect sizes. However, in no region was cortical thickness related to BOLD activation ($ps > .01$; $R^2\Delta < .02$). Gender did not moderate effects.

Conclusions—Cortical thickness, although variable across individuals, was not related to BOLD response, suggesting that structural and functional maturation do not have the same developmental trajectory during early adolescence. These findings are important, as imaging studies that report group differences in regards to cortical thickness should not necessarily assume co-occurring behavioral or functional changes. The methodology used in this study could be of interest to other developmental neuroimaging researchers using multimodal imaging to understand adolescent brain development.

[*]Corresponding author: Lindsay Squeglia, 8950 Villa La Jolla Drive, San Diego, CA 92161, US; telephone: 858-822-2306, fax: 858-552-7414; lsquegli@ucsd.edu..

Keywords

adolescence; cortical thickness; brain activation; BOLD response; normal development; visual working memory

1. INTRODUCTION

Over the past 15 years, a substantial number of structural and functional magnetic resonance imaging (sMRI and fMRI, respectively) studies have shed light on the unique neurodevelopment that occurs during adolescence (Blakemore, 2012; Galván et al., 2012). Significant morphometric and functional brain changes emerge during this developmental period; however, little is known regarding the direct effect of brain structural changes on neural activation and cognitive functioning. Additionally, most imaging studies to date have utilized only one imaging modality when exploring the complex neural development that occurs during this period, limiting the interpretability of the findings. The purpose of this study was to use multimodal imaging (sMRI cortical thickness and fMRI brain activation indices) to examine how structural changes might relate to brain function during adolescence, as surprisingly few studies have addressed this important question.

Intense research efforts have focused on adolescence because of the significant neural development and emergence of psychiatric disorders that occur during this period (Paus et al., 2008). While overall brain volume remains relatively stable during adolescence, gray matter tends to reduce while white matter increases. Gray matter maturation typically follows an inverted U-shaped pattern, with increases in gray matter until early adolescence (roughly peaking at ages 11–13), followed by decreased volume which may relate to the pruning of excess synapses, white matter encroachment, and changes in the extracellular matrix (Paus, 2005) primarily in the prefrontal and temporal cortices (Giedd, 2004; Giedd et al., 2009) and subcortical structures such as the striatum, thalamus, and nucleus accumbens (Huttenlocher, 1990; Sowell et al., 1999). In contrast, white matter continues to increase linearly, well into early adulthood. Increased white matter volume is believed to be related to progressive myelination of axons during adolescence, and is associated with greater connectivity between brain regions (Hüppi and Dubois, 2006; Jernigan and Gamst, 2005; Pfefferbaum et al., 1994; Sowell et al., 2004) and smoother, more efficient communication between frontal-subcortical brain regions (Luna and Sweeney, 2004). Interestingly, cortical regions show developmental specificity, with primary motor and sensory areas reaching peak development (e.g., gray matter decline) first and areas important for higher order cognitive functioning (e.g., dorsolateral prefrontal cortex) developing later in adolescence (Gogtay et al., 2004; Shaw et al., 2008; Sowell et al., 2004).

Dynamic changes in brain structure and activation co-occur during development, but surprisingly little is known about how changes in brain structure relate to changes in brain activity (Lu et al., 2009). Emerging evidence from three different studies on children and adolescents provide preliminary support that cortical thickness is related to brain activation (Lu et al., 2009; Nuñez et al., 2011; Strenziok et al., 2011). Lu and colleagues (Lu et al., 2009) examined 24 children ages 6–15 and found that thinner cortices related to more “mature” activation, meaning “greater” or “less” activation depending on where activation intensity corresponded with skill level improvement . In a sample of 20 adolescents ages 14 to 17, Strenziok and colleagues (2011) found that increased blood oxygen level dependent (BOLD) activation in the prefrontal cortex during an aggression task was associated with thinner cortices in the same region. Nuñez and colleagues (2011) found that thinner inferior frontal cortices were related to greater inferior frontal BOLD activation in children ages 7 to 15 (N=19). Taken together, these multi-modal imaging studies suggest a relationship

between cortical thickness and patterns of brain activation; however, the existing studies have small sample sizes and have explored children and adolescents over a relatively large age range considering the substantial maturation that occurs over short time spans (e.g., months) during adolescence (Sullivan et al., 2011).

Therefore, the purpose of this study was to examine the relationship between cortical thickness and brain activation in a large (N=156) sample of adolescents between ages 12–14 to clarify how brain morphometry is related to neural response. We hypothesized that *thinner* (i.e., more mature) cortices would be associated with *greater* BOLD response, particularly in frontal and parietal regions, during a working memory task (Curtis, 2006). A visual working memory task was chosen to probe this relationship, because tasks of visual working memory evoke substantial activation predominantly in prefrontal and parietal regions (Baker et al., 1996; Courtney et al., 1996; Friedman and Goldman-Rakic, 1994; Haxby et al., 2000; Owen et al., 1996; Petrides et al., 1993), which are areas undergoing significant neurodevelopment during adolescence and are therefore of interest to address our hypothesis. Additionally, the neural substrates of visual working memory have been comprehensively characterized (Cabeza et al., 2004; Cohen et al., 1997; Courtney et al., 1996; Fougnie and Marois, 2006; Postle and D'Esposito, 1999; Smith and Jonides, 1999; Ungerleider et al., 1998) and are easily probed by manipulating the number of items (i.e., load) presented (Luck and Vogel, 1997). Therefore, this task evokes substantial brain activation in areas expected to development during early adolescence (i.e., age 12–14 years), allowing us to clarify the relationship between brain morphometry and brain activation.

2. RESULTS

2.1 Power

A power analysis using G*Power (Faul et al., 2007; Faul et al., 2009) was conducted to determine the sample size needed to detect a small to medium effect size (Cohen's R^2 = . 10), which is the anticipated strength of the relationship between cortical thickness and BOLD response, given our previous structural and functional imaging findings (Squeglia et al., 2012a; Squeglia et al., 2012b). A sample of 132 participants provides a 95% chance of detecting a population R^2 as small as .10 at α =. 05, considering 5 covariates. For our statistical analyses, we had 156 participants available, exceeding the suggested sample size to observe a small to medium effect.

2.2 Age and cortical thickness

Consistent with previous research (Squeglia et al., in press), twelve brain regions showed correspondence between cortical thinning and increasing age between ages 12 to 14, and no region suggested cortical thickening across this period (ps <.05). Regions showing cortical thinning include the right isthmus cingulate [$R^2\Delta$=.03, p=.04; β=−.17], right medial orbitofrontal [$R^2\Delta$=.05, p<.01; β=−.22], right pars orbitalis [$R^2\Delta$=.04, p=.02; β=−.19], right posterior cingulate [$R^2\Delta$=.03, p=.04; β=−.17], right rostral anterior cingulate [$R^2\Delta$=.03, p=. 04; β=−.17], right rostral middle frontal [$R^2\Delta$=.05, p<.01; β=−22], right insula [$R^2\Delta$=.04, p<. 01; β=−21], left medial orbitofrontal [$R^2\Delta$=.03, p=.03; β=−.18], left pars triangularis [$R^2\Delta$=. 04, p=.02; β=−.19], left rostral anterior cingulate [$R^2\Delta$=.05, p<.001; β=−23], left rostral middle frontal [$R^2\Delta$=.02, p=.05; β=−.16], and left insula [$R^2\Delta$=.06, p<.01; β=−.24], controlling for intracranial volume.

2.3 Age and BOLD response

Only one brain region showed correspondence between BOLD response and increasing age between 12 to 14 years of age. *Greater* BOLD response was related to older age in the left temporal pole [$R^2\Delta$=.02, p=.05; β=.16].

2.4 BOLD response to visual working memory task

Overall, 19 brain regions were, on average, positively activated during the 6-dot (high load visual working memory) vs. 2-dot (low load working memory) conditions, encompassing 11 frontal (i.e., left and right caudal anterior cingulate, left and right lateral orbitofrontal, left and right rostral middle frontal, left and right frontal pole, right caudal middle frontal, right pars opercularis, right precentral), two parietal (i.e., left and right superior parietal), four temporal (i.e., left and right fusiform, right entorhinal, right inferior temporal), and two occipital (left and right lateral occipital) regions, as defined by Desikan maps (Desikan et al., 2006). Correlations between each of the 19 ROIs and age, pubertal development, and gender are presented in Tables 2 and 3.

2.5 Cortical thickness and BOLD response

In none of the 19 ROIs was cortical thickness related to BOLD activation, whether or not we considered variability attributable to age, pubertal development, gender, IQ, or intracranial volume (*p*s > .01; $R^2\Delta < .02$). The left frontal pole and right fusiform gyrus showed a positive relationship, where thicker cortices were related to greater BOLD response; however, these findings do not surpass Type I error thresholding (see Table 4). Follow-up exploratory analyses in all other Desikan regions (total: 49 regions) similarly found no relationship between BOLD and cortical thickness (*ps* > .01; $R^2\Delta < .03$).

2.6 Post hoc testing

Because males and females mature at different rates (Giedd et al., 2012), analyses were rerun, adding gender as an interactive term in hierarchical regressions. Gender did not moderate the relationship between cortical thickness and BOLD activation in any of the 19 ROIs (*ps* > .01). Paired-sample t-tests assessed whether there were differences in the variability of imaging indices. For all 68 regions, cortical thickness and BOLD response had similar degrees of variability (*p*s > .05; BOLD: minimum z-score: −3.7, maximum z-score: 3.8; cortical thickness: minimum: −3.8, maximum: 3.7), which is within the acceptable range for analyses (Tabachnick and Fidell, 2007).

3. DISCUSSION

The goals of the present study were to: (1) utilize a novel approach to combining FreeSurfer cortical thickness and AFNI BOLD imaging data and (2) to elucidate the relationship between structural and functional imaging indices during adolescence. In a group of 156 healthy adolescents between the ages 12 and 14, we found that cortical thinning during this period was not related to BOLD response, suggesting that structural and functional maturation do not have the same developmental trajectory during early adolescence. To our knowledge, the methodology used in this study to align sMRI and fMRI has not been previously reported.

Despite power analyses suggesting adequate power to detect effects, none of the brain regions examined showed an association between cortical thickness and BOLD response, suggesting gray matter and brain activation maturation have different developmental trajectories during early adolescence. These findings are important, as imaging studies that report structural group differences, particularly in regards to cortical thickness, should not necessarily assume these differences are associated with behavioral or functional changes. Continued white matter maturation, which was not assessed in this study, might help explain the disconnect between cortical thinning and brain activation. Myelination of axons continues well into adulthood, and is associated with greater structural connectivity between brain regions (Hüppi and Dubois, 2006; Jernigan and Gamst, 2005; Pfefferbaum et al., 1994; Sowell et al., 2004) and smoother, more efficient communication between frontal-

subcortical brain regions (Luna and Sweeney, 2004). Therefore, increasing myelination may help better explain brain activation patterns during neurodevelopment than cortical thinning. Future studies that take into account both gray and white matter maturation will be important in elucidating structure-function relationships.

There is surprisingly limited research on the relationship between brain structure and function. Previous studies with children and adolescents have found that cortical thinning is associated with both *greater* and *less* BOLD activation (Lu et al., 2009; Nuñez et al., 2011; Strenziok et al., 2011). Discrepancies between studies may be due to the age ranges studied, which included younger children and older adolescents, as well as different tasks utilized. In our study, we were examining a restricted age range (between 12–14) to reduce developmental heterogeneity in cortical thickness and BOLD indices, which may have limited our ability to detect effects that might be occurring over a more protracted period of time. Additional analyses examined the degree of variability present in the different imaging indices. Both cortical thickness and BOLD response had similar levels of variability for all regions. Therefore, findings were not influenced by greater variability in measurement between imaging indices.

Limitations of this study include the cross-sectional nature of the data, precluding any casual interpretations. The age range of our study was limited between ages 12–14 to reduce heterogeneity in brain development expected over adolescence; therefore, we cannot generalize findings to children, older adolescents, or adults. By averaging BOLD and cortical thickness across predefined anatomical regions (Desikan et al., 2006), it is possible that smaller, more localized relationships between structure and function were missed. The Desikan atlas was chosen because it provides regions that are anatomically and functionally similar, without parcellating the brain into a large number of small regions that would result in Type I error concerns. Despite these limitations, notable strengths are that this study used multimodal imaging and novel alignment methodology to better understand the relationship between structural and functional brain development during adolescence in a large sample size of a focused age range. Future studies should employ additional neuroimaging indices, including diffusion tensor imaging, to clarify the effect of myelination on BOLD response. These findings suggest that cortical thinning during adolescence may not be directly related to brain activation patterns. The methodology used in this study could be of interest to other developmental neuroimaging researchers who are using multimodal imaging to understand adolescent brain development.

4. MATERIALS AND METHODS

4.1 Participants

Participants were 156 healthy 12–14 year-olds (44% female) recruited through flyers sent to households of students attending local middle schools. Extensive screening and background information were obtained from the youth, their biological parent, and one other parent or close relative. The study protocol was executed in accordance with the standards approved by the University of California, San Diego Human Research Protections Program.

Exclusionary criteria were: any neurological or DSM-IV (American Psychiatric Association, 2000) Axis I disorder, determined by the NIMH Diagnostic Interview Schedule for Children –version 4.0 (Shaffer et al., 2000); head trauma or loss of consciousness (>2 minutes); history of chronic medical illness; learning disability or mental retardation; use of medications potentially affecting the brain; premature birth (i.e., born prior to 35th gestational week); any suggestion of prenatal alcohol (>2 drinks during a given week) or illicit drug exposure; experience with alcohol or drugs, defined as >10 total days in their life on which drinking had occurred, or > 2 drinks in a week; >1 lifetime experiences with

marijuana and any use in the past three months; >5 lifetime cigarette uses (Squeglia et al., 2009; Squeglia et al., 2012a); any history of other intoxicant use; contraindication to MRI (e.g., braces); inadequate comprehension of English; and non-correctable sensory problems. The final sample (*N*=156) contained 35 12-year-olds (54% female), 80 13-year-olds (43% female), and 41 14-year-olds (37% female) (see Table 1), typically in 7th grade, with modal family socioeconomic status in the Hollingshead (Hollingshead, 1965) 11–15 range, and commonly with high average estimated IQ and school grades.

4.2 Measures

4.2.1 Neurocognition—The Vocabulary subtest of the Wechsler Abbreviated Scale of Intelligence (Wechsler, 1999) was administered by trained psychometrists to estimate verbal IQ.

4.2.2 Pubertal Development—The Pubertal Development Scale (Petersen et al., 1988) ascertained current level of pubertal development with five sex-specific items.

4.3 Procedures

4.3.1 Image acquisition—High-resolution anatomical and functional images were collected at the UC San Diego Center for fMRI during the same scan session on a 3-Tesla CXK4 short bore Excite-2 MR system (General Electric, Milwaukee, WI) with an 8-channel phase-array head coil. Participants were placed comfortably on the scanner table and the head was stabilized within the head coil using foam cushions (NoMoCo Pillow, La Jolla, CA). Scan sessions involved a 10-second scout scan to assure good head placement and slice selection covering the whole brain followed by a high-resolution T1-weighted sequence using a sagittally acquired spoiled gradient recalled sequence (FOV 24 cm, 256 × 256 x 192 matrix, .94 x .94 × 1 mm voxels, 176 slices, TR=20 ms, TE=4.8 ms; flip angle 12°, acquisition time 7:26 minutes). BOLD response contrast was measured with T2*-weighted axially acquired echo-planar images (FOV=24 cm, 64 × 64 matrix, 3.75 × 3.75 × 3.8 mm voxels, 32 slices, TE=30 ms, TR=2000 ms, flip angle 90°, ramped bandwidth 250 KHz). Field maps were acquired to minimize warping and signal dropout (~4 minutes total) and employed 2 different echo times to assess field inhomogeneities and signal distortions under the same grid parameters as echo-planar images were acquired.

4.3.2 Task—All participants were administered the same fast event related visual working memory task (Paulus et al., 2006; Tapert et al., 2004) during fMRI acquisition. Each trial consisted of an array of 2, 4, or 6 colored dots briefly (100 ms) presented against a gray background. Because previous research showed that 3 to 4 different items can be held simultaneously in visual working memory (Luck and Vogel, 1997), this task used the 2-dot array as the low capacity condition, 4-dot as mid-capacity, and 6-dot as the high or supra-capacity condition. After a 1000 ms delay, the subsequent trial (2000 ms) included the same number of dots presented in the same location and were either the same color-array or one color different. For each trial, the subjects pressed button “1” if color displays were the same and “2” if they differed. This was followed by a 500 ms timeout; 50% of the trials had identical color arrays, while 50% had a one-color dot difference. Each subject completed 30 trials of each type (2, 4, or 6 dots) presented randomly, in addition to 69 null trials of 2000 ms each interspersed to provide an optimized fast-event related sequence (256 repetitions in all). The task lasted 8 minutes and 32 seconds. The 6-dot condition is considered supra-span (i.e., higher than most people’s working memory span) and of the 2-dot condition is sub-span (i.e., well within most people’s working memory load capacity (Luck and Vogel, 1997). None of the 156 total runs used during analysis had performance at or below chance level (50%) on the 2-dot (i.e., low-capacity/easy condition; see Figure 1). fMRI task stimuli were back-projected from a laptop to a screen at the foot of the scanner bed visible via an

angled mirror attached to the head coil. Accuracy and reaction time data were logged with a fiber-optic response box (Current Designs, Pittsburgh, PA). The primary outcome measure was BOLD response contrast to 6-dot (supra-span) relative to 2-dot (sub-span) conditions (see Table 1 for task performance data).

4.4 Data Analysis

4.4.1 Structural image processing—FreeSurfer (version 5.0, surfer.nmr.mgh.harvard.edu) was used for cortical surface reconstruction and cortical thickness estimation (Dale et al., 1999; Fischl et al., 1999). The FreeSurfer program utilizes a series of automated imaging algorithms to produce measures of cortical thickness. The process first involves intensity normalization, skull-stripping, and labeling of the subcortical white and deep gray matter volumetric structures. The white matter border is then tessellated by placing two triangles at each face (square) that separates white matter voxels from other voxels (i.e., gray matter). This initial coarse tessellation is then smoothed via surface deformation algorithm, guided by local MRI intensity gradients to optimally place smooth gray/white and, by deforming outward, gray/cerebrospinal fluid borders at the location where the greatest shift in intensity defines the transition to the other tissue class (Dale et al., 1999; Fischl et al., 1999; Fischl and Dale, 2000; Fischl et al., 2004). The smoothing produced from the spatial intensity gradients across tissue classes frees the surfaces from being reliant on the absolute signal intensity. Thus, this surface rendering process yields data that are not constrained to the voxel resolution of the original images, allowing for the quantification of submillimeter group differences (Fischl and Dale, 2000). Cortical thickness was calculated as the closest distance from the gray/white matter boundary to the gray matter/cerebral spinal fluid boundary at each vertex on the cortical surface (Fischl and Dale, 2000). The validity of the cortical thickness measurement procedures has been verified using manual measurements (Kuperberg et al., 2003; Salat et al., 2004) and histological analysis (Rosas et al., 2002).

One rater (LMS), blind to participant characteristics, followed the reconstruction procedures (http://surfer.nmr.mgh.harvard.edu/fswiki/RecommendedReconstruction) to identify and correct any errors made during the cortical reconstruction. Four participants (not described in this paper) had unusable data due to excessive motion and were discarded. This involved verification of the automated skull stripping, as well as a coronal plane slice-by-slice inspection of the gray/white and gray/cerebrospinal fluid surfaces. Modifications to the surfaces were made as necessary to correct for tissue misclassifications (e.g., residual dura matter classified as cortex). Following inspection, an automated parcellation procedure divided each hemisphere into 32 independent cortical regions based on gyral and sulcal features (Desikan et al., 2006; Fischl et al., 2004). Cortical thickness estimates of each region were extracted for subsequent statistical analyses.

4.4.2 Functional image processing—Analysis of Functional NeuroImages (AFNI; (Cox, 1996) was used to process functional images. Artifact and aberrant signal levels were examined in each repetition of each slice using an automated program developed by the UCSD Laboratory of Cognitive Neuroimaging. Motions in time series data were corrected by registering each acquisition to the maximally stable base volume with an iterated least squares algorithm (Cox and Jesmanowicz, 1999) to estimate 3 rotational and 3 displacement parameters for each participant. An output file specifying adjustments made controlled for spin history effects (Bandettini et al., 1993; Friston et al., 1996) in analyses if no significant task-correlated motion was found. To evaluate task-related motion, the reference vector was correlated with the 6 motion parameters for each dataset. Datasets with significant task-correlated or bulk motion were excluded from analyses. Two trained raters then scanned the time series *en cine* to omit any remaining repetitions with visually discernible motion; if

more than 15% of repetitions in a task were discarded, the run was not used (n=10, not described in this paper).

Raw time series data were standardized to percent signal change from baseline, and deconvolution was conducted with a reference function that convolved the behavioral stimuli with a hemodynamic response model (Cohen et al., 1997), while covarying for linear trends and motion correction, ignoring the first 3 repetitions. This resulted in a functional image in which every voxel contains a fit coefficient representing the change in signal across behavioral conditions, as well as percent signal change and threshold statistics. Standardization transformations were made for each high-resolution anatomical image (Talairach and Tournoux, 1988), and functional datasets were warped in accordance to manage individual anatomical variability. Functional data were resampled into isotropic voxels (3 mm^3), and a spatial smoothing Gaussian filter (full-width half maximum 5 mm) was applied to minimize the influence of individual anatomic variability. Co-registration of structural images to functional images was performed with a mutual information registration program (Cox and Jesmanowicz, 1999) that robustly handles images with different signal characteristics and of different spatial resolutions.

4.4.3 Volumetric and functional image alignment—The AFNI SUrface MApper (SUMA; (Saad and Reynolds, 2012) program was used to align segmented volumetric and functional datasets to the same template space. SUMA programs allow for fine control over the mapping between volume and surface domains produced by the FreeSurfer segmentation process while maintaining a direct link to volumetric data from which surface models and data originated. First, segmented volumetric data produced by FreeSurfer were aligned to the same original space as the functional data and a rater checked the correspondence between datasets to ensure proper alignment. Next, volumetric data were warped to standard atlas space (Talairach and Tournoux, 1988) using the same algorithm as in the previous functional and structural data steps, and resampled to 3 mm^3 voxels to match the functional data. Thus, the 68 independent cortical gray matter regions (Desikan et al., 2006) produced during the segmentation process served as individualized specific regions of interest (ROI) from which mean BOLD values were extracted for subsequent analyses (see Figure 2).

The functional outcome of interest was the BOLD response contrast comparing the 6-dot array relative to the 2-dot array (high load versus low load condition), interpreted as brain response to increasing working memory load. A greater BOLD response contrast (i.e., larger fit coefficient) was interpreted as more cognitive energy to complete the challenging supra-span (6-dot) trials. BOLD response values, averaged across the parcellation regions derived from FreeSurfer (Desikan et al., 2006), were imported from AFNI to SPSS. The volumetric outcome was cortical thickness values, averaged across each parcellation region (Desikan et al., 2006), which were imported from FreeSurfer to SPSS (Rel. 18.0.0. 2009. IBM, Chicago, IL) for each participant.

4.5 Statistical Analyses

4.5.1 Age and cortical thickness—Hierarchical linear regressions were run to determine the effect of age on cortical thickness. Age was entered as the independent variable, and cortical thickness in each ROI was entered as the dependent variable. Intracranial volume was controlled as a covariate.

4.5.2 Age and BOLD response—Hierarchical linear regressions were run to determine the effect of age on BOLD response. Age was entered as the independent variable, and BOLD response contrast in each ROI was entered as the dependent variable.

4.5.3 BOLD response to visual working memory task—BOLD response averages for the 6-dot (high working memory load) to the 2-dot (low working memory load) contrast were extracted from each Desikan region (Desikan et al., 2006). Regions that had positive average values (i.e., regions activated more during the high vs. low working memory load) were used as regions of interest.

4.5.4 Cortical thickness and BOLD response—Hierarchical linear regressions were run to determine the effect of cortical thickness on visual working memory BOLD response contrast in the 19 ROIs (through FreeSurfer segmentations) that were consistently activated during the visual working memory task. Cortical thickness for each ROI was entered as the independent variable and BOLD response in the corresponding ROI was entered as the dependent variable, covarying for age, pubertal development, gender, IQ, and intracranial volume.

5. CONCLUSIONS

Cortical thickness, although variable across individuals, was not related to BOLD response, suggesting that structural and functional maturation do not have the same developmental trajectory during early adolescence. These findings are important, as imaging studies that report group differences in regards to cortical thickness should not necessarily assume co-occurring behavioral or functional changes. The methodology used in this study could be of interest to other developmental neuroimaging researchers using multimodal imaging to understand adolescent brain development. Future research employing white matter integrity indices could help elucidate the relationship between structural and functional maturation during adolescence.

Acknowledgments

This research was supported by grants from the National Institute of Alcohol Abuse and Alcoholism (R01 AA13419 to Tapert; F32 AA021610 to Squeglia) and the National Institute of Drug Abuse (F32 DA032188 to Jacobus).

Special thanks to thanks to the Adolescent Brain Imaging Project lab: M. J. Meloy, Ph.D., Sonja Eberson, M.A., Katy Bever, Feras Tartir, Zachary Lew, Ashley Tracas, and Komol Kapoor and the participating schools in the San Diego Unified School District and their families.

Funding Support: R01 AA13419 (PI: Tapert), F32 AA021610 (PI: Squeglia), and F32 DA032188 (PI: Jacobus).

References

American Psychiatric Association. Diagnostic and statistical manual of mental disorders. 4th ed., text revision. Washington, DC: 2000. Vol

Baker SC, Frith CD, Frackowiak RS, Dolan RJ. Active representation of shape and spatial location in man. Cerebral Cortex. 1996; 6:612–619. [PubMed: 8670686]

Bandettini PA, Jesmanowicz A, Wong EC, Hyde JS. Processing strategies for time-course data sets in functional MRI of the human brain. Magnetic Resonance in Medicine. 1993; 30:161–173. [PubMed: 8366797]

Blakemore SJ. Imaging brain development: the adolescent brain. NeuroImage. 2012; 61:397–406. [PubMed: 22178817]

Cabeza R, Daselaar SM, Dolcos F, Prince SE, Budde M, Nyberg L. Task-independent and task-specific age effects on brain activity during working memory, visual attention and episodic retrieval. Cerebral Cortex. 2004; 14:364–375. [PubMed: 15028641]

Cohen JD, Perlstein WM, Braver TS, Nystrom LE, Noll DC, Jonides J, Smith EE. Temporal dynamics of brain activation during a working memory task. Nature. 1997; 386:604–608. [PubMed: 9121583]

Courtney SM, Ungerleider LG, Keil K, Haxby JV. Object and spatial visual working memory activate separate neural systems in human cortex. Cerebral Cortex. 1996; 6:39–49. [PubMed: 8670637]

Cox RW. AFNI: Software for analysis and visualization of functional magnetic resonance neuroimages. Computers and Biomedical Research. 1996; 29:162–173. [PubMed: 8812068]

Cox RW, Jesmanowicz A. Real-time 3D image registration for functional MRI. Magnetic Resonance in Medicine. 1999; 42:1014–1018. [PubMed: 10571921]

Curtis CE. Prefrontal and parietal contributions to spatial working memory. Neuroscience. 2006; 139:173–180. [PubMed: 16326021]

Dale AM, Fischl B, Sereno MI. Cortical surface-based analysis. I. Segmentation and surface reconstruction. NeuroImage. 1999; 9:179–194. [PubMed: 9931268]

Desikan RS, Segonne F, Fischl B, Quinn BT, Dickerson BC, Blacker D, Buckner RL, Dale AM, Maguire RP, Hyman BT, Albert MS, Killiany RJ. An automated labeling system for subdividing the human cerebral cortex on MRI scans into gyral based regions of interest. NeuroImage. 2006; 31:968–980. [PubMed: 16530430]

Faul F, Erdfelder E, Lang A-G, Buchner A. G*Power 3: A flexible statistical power analysis program for the social, behavioral, and biomedical sciences. Behavior Research Methods. 2007; 39:175–191. [PubMed: 17695343]

Faul F, Erdfelder E, Buchner A, Lang A-G. Statistical power analyses using G*Power 3.1: Tests for correlation and regression analyses. Behavior Research Methods. 2009; 41:1149–1160. [PubMed: 19897823]

Fischl B, Sereno MI, Dale AM. Cortical surface-based analysis. II: Inflation, flattening, and a surface-based coordinate system. NeuroImage. 1999; 9:195–207. [PubMed: 9931269]

Fischl B, Dale AM. Measuring the thickness of the human cerebral cortex from magnetic resonance images. Proceedings of the National Academy of Sciences of the United States of America. 2000; 97:11050–11055. [PubMed: 10984517]

Fischl B, van der Kouwe A, Destrieux C, Halgren E, Segonne F, Salat DH, Busa E, Seidman LJ, Goldstein J, Kennedy D, Caviness V, Makris N, Rosen B, Dale AM. Automatically parcellating the human cerebral cortex. Cerebral Cortex. 2004; 14:11–22. [PubMed: 14654453]

Fougnie D, Marois R. Distinct capacity limits for attention and working memory: Evidence from attentive tracking and visual working memory paradigms. Psychological Science. 2006; 17:526–534. [PubMed: 16771804]

Friedman HR, Goldman-Rakic PS. Coactivation of prefrontal cortex and inferior parietal cortex in working memory tasks revealed by 2DG functional mapping in the rhesus monkey. Neuroscience. 1994; 14:2775–2788. [PubMed: 8182439]

Friston KJ, Williams S, Howard R, Frackowiak RSJ, Turner R. Movement-related effects in fMRI time-series. Magnetic Resonance in Medicine. 1996; 35:346–355. [PubMed: 8699946]

Galván A, Van Leijenhorst L, McGlennen KM. Considerations for imaging the adolescent brain. Developmental Cognitive Neuroscience. 2012; 2:293–302. [PubMed: 22669033]

Giedd JN. Structural magnetic resonance imaging of the adolescent brain. Annals of the New York Academy of Sciences. 2004; 1021:77–85. [PubMed: 15251877]

Giedd JN, Lalonde FM, Celano MJ, White SL, Wallace GL, Lee NR, Lenroot RK. Anatomical brain magnetic resonance imaging of typically developing children and adolescents. Journal of American Academy of Child & Adolescent Psychiatry. 2009; 48:465–470.

Giedd JN, Raznahan A, Mills KL, Lenroot RK. Review: Magnetic resonance imaging of male/female differences in human adolescent brain anatomy. Biology of Sex Differences. 2012; 3:19. [PubMed: 22908911]

Gogtay N, Giedd JN, Lusk L, Hayashi KM, Greenstein D, Vaituzis AC, Nugent TFr, Herman DH, Clasen LS, Toga AW, Rapoport JL, Thompson PM. Dynamic mapping of human cortical development during childhood through early adulthood. Proceedings of the National Academy of Sciences. 2004; 101:8174–8179.

Haxby JV, Petit L, Ungerleider LG, Courtney SM. Distinguishing the functional roles of multiple regions in distributed neural systems for visual working memory. NeuroImage. 2000; 11:380–391. [PubMed: 10806025]

Hollingshead, AB. Two-factor index of social position. New Haven, CT: Yale University Press; 1965. Vol

Hüppi PS, Dubois J. Diffusion tensor imaging of brain development. Seminars in Fetal and Neonatal Medicine. 2006; 11:489–497. [PubMed: 16962837]

Huttenlocher PR. Morphometric study of human cerebral cortex development. Neuropsychologia. 1990; 28:517–527. [PubMed: 2203993]

Jernigan TL, Gamst AC. Changes in volume with age-consistency and interpretation of observed effects. Neurobiology of Aging. 2005; 26:1271–1274. discussion 1275-1278. [PubMed: 16006011]

Kuperberg GR, Broome MR, McGuire PK, David AS, Eddy M, Ozawa F, Goff D, West WC, Williams SC, van der Kouwe AJ, Salat DH, Dale AM, Fischl B. Regionally localized thinning of the cerebral cortex in schizophrenia. Archives of General Psychiatry. 2003; 60:878–888. [PubMed: 12963669]

Lu LH, Dapretto M, O'Hare ED, Kan E, McCourt ST, Thompson PM, Toga AW, Bookheimer SY, Sowell ER. Relationships between brain activation and brain structure in normally developing children. Cerebral Cortex. 2009; 19:2595–2604. [PubMed: 19240138]

Luck SJ, Vogel EK. The capacity of visual working memory for features and conjunctions. Nature. 1997; 390:279–281. [PubMed: 9384378]

Luna B, Sweeney JA. The emergence of collaborative brain function: fMRI studies of the development of response inhibition. Annals of the New York Academy of Sciences. 2004; 1021:296–309. [PubMed: 15251900]

Nuñez SC, Dapretto M, Katzir T, Starr A, Bramen J, Kan E, Bookheimer S, Sowell ER. fMRI of syntactic processing in typically developing children: Structural correlates in the inferior frontal gyrus. Developmental Cognitive Neuroscience. 2011; 1:313–323. [PubMed: 21743820]

Owen AM, Morris RG, Sahakian BJ, Polkey CE, Robbins TW. Double dissociations of memory and executive functions in working memory tasks following frontal lobe excisions, temporal lobe excisions or amygdalo-hippocampectomy in man. Brain. 1996; 119:1597–1615. [PubMed: 8931583]

Paulus MP, Tapert SF, Pulido C, Schuckit MA. Alcohol attenuates load-related activation during a working memory task: Relation to level of response to alcohol. Alcoholism: Clinical and Experimental Research. 2006; 30:1363–1371.

Paus T. Mapping brain maturation and cognitive development during adolescence. Trends in Cognitive Science. 2005; 9:60–68.

Paus T, Keshavan M, Giedd JN. Why do many psychiatric disorders emerge during adolescence? Nature Reviews. Neuroscience. 2008; 9:947–957. [PubMed: 19002191]

Petersen AC, Crockett L, Richards M, Boxer A. A self-report measure of pubertal status: Reliability, validity, and initial norms. Journal of Youth and Adolescence. 1988; 17

Petrides M, Alivisatos B, Evans AC, Meyer E. Dissociation of human mid-dorsolateral from posterior dorsolateral frontal cortex in memory processing. Proceedings of the National Academy of Sciences. 1993; 90:873–877.

Pfefferbaum A, Mathalon DH, Sullivan EV, Rawles JM, Zipursky RB, Lim KO. A quantitative magnetic resonance imaging study of changes in brain morphology from infancy to late adulthood. Archives of Neurology. 1994; 51:874–887. [PubMed: 8080387]

Postle BR, D'Esposito M. "What"-Then-Where" in visual working memory: An event-related fMRI study. Journal of Cognitive Neuroscience. 1999; 11:585–597. [PubMed: 10601740]

Rosas HD, Liu AK, Hersch S, Glessner M, Ferrante RJ, Salat DH, van der Kouwe A, Jenkins BG, Dale AM, Fischl B. Regional and progressive thinning of the cortical ribbon in Huntington's disease. Neurology. 2002; 58:695–701. [PubMed: 11889230]

Saad ZS, Reynolds RC. SUMA. NeuroImage. 2012; 62:768–773. [PubMed: 21945692]

Salat DH, Buckner RL, Snyder AZ, Greve DN, Desikan RS, Busa E, Morris JC, Dale AM, Fischl B. Thinning of the cerebral cortex in aging. Cerebral Cortex. 2004; 14:721–730. [PubMed: 15054051]

Shaffer D, Fisher P, Lucas CP, Dulcan MK, Schwab-Stone ME. NIMH Diagnostic Interview Schedule for Children Version IV (NIMH DISC-IV): Description, differences from previous versions, and

reliability of some common diagnoses. Journal of the American Academy of Child and Adolescent Psychiatry. 2000; 39:28–38. [PubMed: 10638065]

Shaw P, Kabani NJ, Lerch JP, Eckstrand K, Lenroot R, Gogtay N, Greenstein D, Clasen L, Evans A, Rapoport JL, Giedd JN, Wise SP. Neurodevelopmental trajectories of the human cerebral cortex. Journal of Neuroscience. 2008; 28:3586–3594. [PubMed: 18385317]

Smith EE, Jonides J. Storage and executive processes in the frontal lobes. Science. 1999; 283:1657–1661. [PubMed: 10073923]

Sowell ER, Thompson PM, Holmes CJ, Jernigan TL, Toga AW. In vivo evidence for post adolescent brain maturation in frontal and striatal regions. Nature Neuroscience. 1999; 2:859–861.

Sowell ER, Thompson PM, Leonard CM, Welcome SE, Kan E, Toga AW. Longitudinal mapping of cortical thickness and brain growth in normal children. Journal of Neuroscience. 2004; 24:8223–8231. [PubMed: 15385605]

Squeglia LM, Spadoni AD, Infante MA, Myers MG, Tapert SF. Initiating moderate to heavy alcohol use predicts changes in neuropsychological functioning for adolescent girls and boys. Psychology of Addictive Behaviors. 2009; 23:715–722. [PubMed: 20025379]

Squeglia LM, Pulido C, Wetherill RR, Jacobus J, Brown GG, Tapert SF. Brain response to working memory over three years of adolescence: Influence of initiating heavy drinking. Journal of Studies on Alcohol and Drugs. 2012a; 73:749–760. [PubMed: 22846239]

Squeglia LM, Sorg SF, Schweinsburg AD, Wetherill RR, Pulido C, Tapert SF. Binge drinking differentially affects adolescent male and female brain morphometry. Psychopharmacology. 2012b; 220:529–539. [PubMed: 21952669]

Squeglia LM, Jacobus J, Sorg SF, Jernigan TL, Tapert SF. Early adolescent cortical thinning is related to better neuropsychological performance. Journal of the International Neuropsychological Society. in press.

Strenziok M, Krueger F, Heinecke A, Lenroot RK, Knutson KM, van der Meer E, Grafman J. Developmental effects of aggressive behavior in male adolescents assessed with structural and functional brain imaging. Social Cognitive and Affective Neuroscience. 2011; 6:2–11. [PubMed: 19770220]

Sullivan EV, Pfefferbaum A, Rohlfing T, Baker FC, Padilla ML, Colrain IM. Developmental change in regional brain structure over 7 months in early adolescence: comparison of approaches for longitudinal atlas-based parcellation. NeuroImage. 2011; 57:214–224. [PubMed: 21511039]

Tabachnick, BG.; Fidell, LS. Using multivariate statistics. Pearson, Boston: 2007. Vol

Talairach, J.; Tournoux, P. Coplanar stereotaxic atlas of the human brain. Three-dimensional proportional system: An approach to cerebral imaging. Thieme, New York: 1988. Vol

Tapert SF, Pulido C, Paulus MP, Schuckit MA, Burke C. Level of response to alcohol and brain response during visual working memory. Journal of Studies on Alcohol. 2004; 65:692–700. [PubMed: 15700505]

Ungerleider LG, Courtney SM, Haxby JV. A neural system for human visual working memory. Proceedings of the National Academy of Sciences of the United States of America. 1998; 95:883–890. [PubMed: 9448255]

Highlights

1. We introduce novel registration techniques for structural and functional MRI data.
2. Cortical thickness is not related to brain activation in 12–14 year old adolescents.
3. Multimodal imaging registration techniques help clarify brain development trajectories.

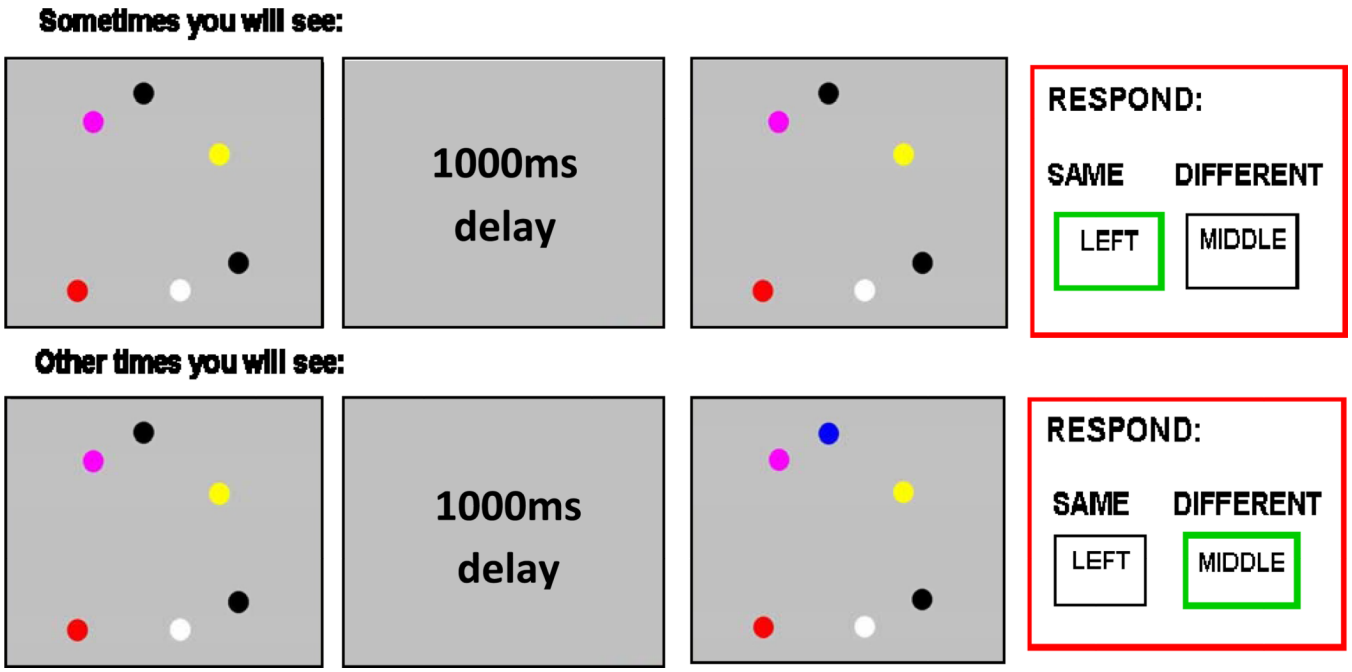

Figure 1.
Visual working memory task. The 6-dot (high working memory load) vs. 2 dot (low working memory load) BOLD response contrast was used in analyses.

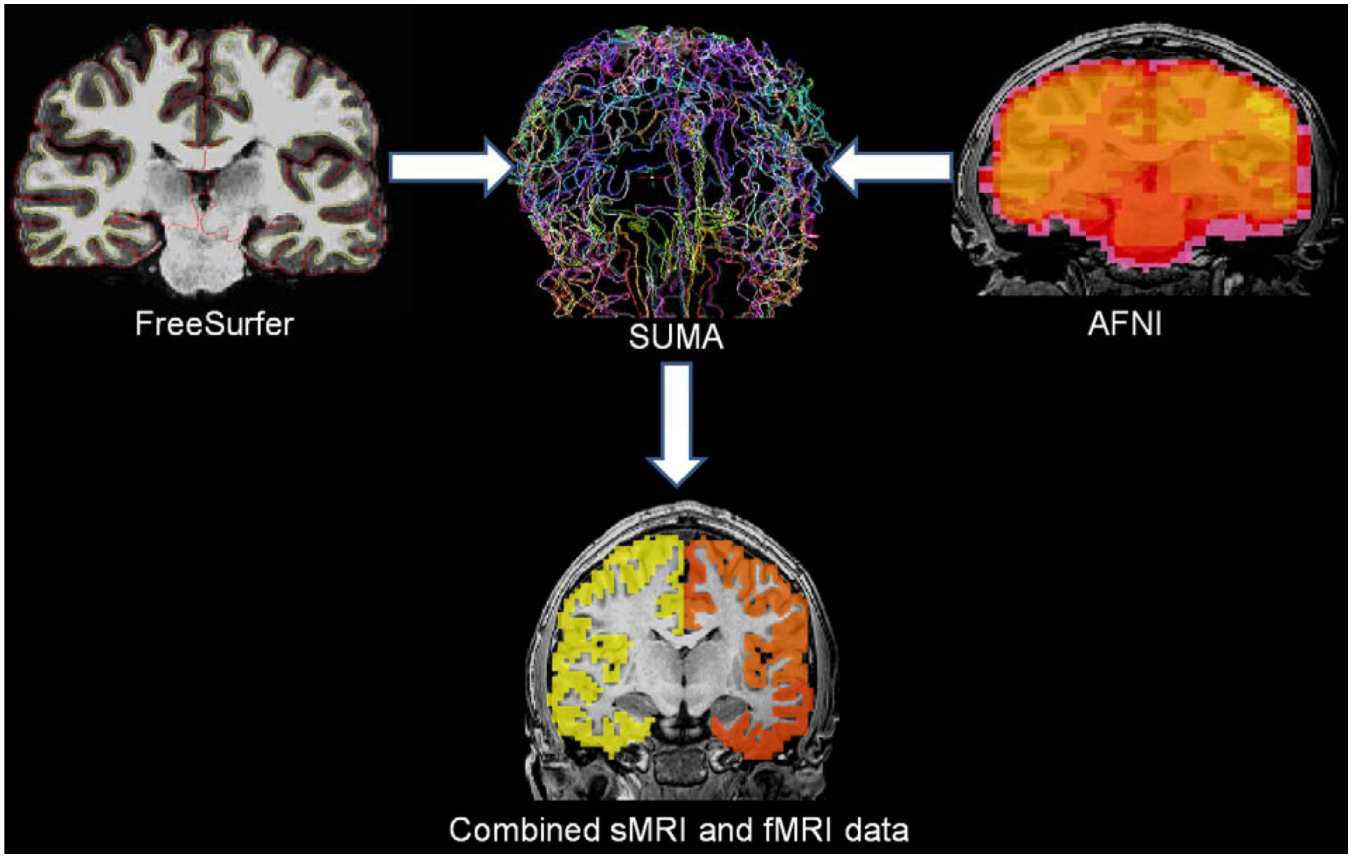

Figure 2.
Graphic depiction of the steps used to combine FreeSurfer cortical thickness structual MRI (sMRI) and Analysis of Functional NeuroImages (AFNI) functional magnetic resonance imaging (fMRI) data. Surface Mapper (SUMA; colored lines correspond to brain region parcellations) combines FreeSurfer and AFNI data and extracts brain activation within each FreeSurfer defined region of interest (yellow and orange images indicate areas where BOLD activation is extracted).

Table 1

Demographic and performance information for participants (*N*=156).

	Mean (SD)
Age (range: 12–14)	13.5 (0.7)
Gender (% Females)	44%
Race (% Caucasian)	68%
Hollingshead Index of Social Position score	22.7 (14.4)
Years of education completed	6.9 (0.8)
Females' Pubertal Development Scale total	14.8 (3.2)
Males' Pubertal Development Scale total	10.9 (3.0)
Grade point average	3.5 (0.5)
WASI Vocabulary T-score	57.1 (8.9)
Visual working memory task performance:	
2 dot accuracy (% correct)	93.1 (8)
6 dot accuracy (% correct)	75.8 (11)
2 dot reaction time (ms)	2390 (208)
6 dot reaction time (ms)	2539 (202)

Table 2

Correlations (*r*) between age, pubertal development, gender, and **cortical thickness** in regions of interest.

Frontal lobe (11 regions)	Age	PDS	Gender
Left caudal anterior cingulate	−.16	.00	−.20*
Right caudal anterior cingulate	−.05	.03	−.18*
Left lateral orbitofrontal	−.15	−.11	.08
Right lateral orbitofrontal	−.08	−.05	.03
Left rostral middle frontal	−.15	−.14	−.01
Right rostral middle frontal	−.26**	−.10	−.120
Left frontal pole	−.09	.06	−.08
Right frontal pole	−.14	−.04	−.05
Right caudal middle frontal	−.12	−.10	−.22**
Right pars opercularis	−.12	−.06	−.04
Right precentral	.04	.03	−.14
Parietal lobe (2 regions)			
Left superior parietal	−.03	−.12	.01
Right superior parietal	−.09	−.05	−.09
Temporal lobe (4 regions)			
Left fusiform	−.06	−.08	.01
Right fusiform	−.01	−.17*	.04
Right entorhinal	−.02	.12	−.08
Right inferior temporal	−.17*	−.10	−.07
Occipital lobe (2 regions)			
Left lateral occipital	−.03	−.10	.04
Right lateral occipital	−.05	−.09	.04

* $p < .05$

** $p < .01$; PDS=Pubertal Development Scale total score; Gender coded as: 0 female, 1 male

Table 3

Correlations (*r*) between age, gender, pubertal development, and **BOLD response** in regions of interest. Note: No regions showed significant relationships between age, pubertal development, orgender and BOLD response (*p*s > .05).

Frontal lobe (11 regions)	**Age**	**PDS**	**Gender**
Left caudal anterior cingulate	−.07	.07	−.08
Right caudal anterior cingulate	−.03	.09	−.07
Left lateral orbitofrontal	.03	.06	.04
Right lateral orbitofrontal	.01	.04	.02
Left rostral middle frontal	.01	.00	.00
Right rostral middle frontal	−.01	−.01	.00
Left frontal pole	.06	−.03	.11
Right frontal pole	.07	.04	.04
Right caudal middle frontal	−.04	.00	.01
Right pars opercularis	−.07	.01	−.01
Right precentral	−.02	.04	.01
Parietal lobe (2 regions)			
Left superior parietal	.02	.00	.07
Right superior parietal	−.04	.05	−.07
Temporal lobe (4 regions)			
Left fusiform	−.05	.05	.00
Right fusiform	−.06	.02	.03
Right entorhinal	.03	.01	−.06
Right inferior temporal	.07	.04	.10
Occipital lobe (2 regions)			
Left lateral occipital	.02	−.03	.05
Right lateral occipital	.00	−.09	.02

* *p* <.05

** *p* <.01; PDS=Pubertal Development Scale total score; Gender coded as: 0 female, 1 male

Table 4

Average BOLD response (high load 6-dot vs. low load 2-dot working memory) and cortical thickness in each region of interest and correlation between BOLD and cortical thickness (*r* and *p*). The left frontal pole and and right fusiform show significant positive correlations ($p < .05$); however, these findings do not surpass Type I error correction.

Frontal lobe (11 regions)	**BOLD response contrast (% signal change) M (SD)**	**Cortical thickness (mm) M (SD)**	***r***	***p***
Left caudal anterior cingulate	0.55 (4.70)	2.99 (0.29)	.04	.67
Right caudal anterior cingulate	1.59 (4.88)	2.86 (0.26)	.06	.48
Left lateral orbitofrontal	0.18 (2.46)	2.75 (0.16)	.06	.47
Right lateral orbitofrontal	0.46 (2.87)	2.82 (0.16)	.03	.69
Left rostral middle frontal	0.45 (4.04)	2.51 (0.12)	.05	.51
Right rostral middle frontal	1.49 (4.71)	2.51 (0.11)	.09	.27
Left frontal pole	**0.41 (6.41)**	**3.19 (0.34)**	**.15**	**.05***
Right frontal pole	0.78 (5.57)	3.05 (0.32)	.09	.26
Right caudal middle frontal	0.36 (4.33)	2.80 (0.15)	.05	.56
Right pars opercularis	1.16 (4.94)	2.90 (0.17)	−.01	.93
Right precentral	0.06 (3.25)	2.75 (0.13)	−.04	.62
Parietal lobe (2 regions)				
Left superior parietal	2.79 (4.99)	2.58 (0.12)	.08	.34
Right superior parietal	4.32 (5.37)	2.57 (0.12)	−.09	.25
Temporal lobe (4 regions)				
Left fusiform	2.01 (3.46)	3.07 (0.12)	−.05	.51
Right fusiform	**2.54 (3.96)**	**3.06 (0.12)**	**.18**	**.03***
Right entorhinal	0.27 (3.10)	3.66 (0.35)	−.10	.21
Right inferior temporal	0.15 (2.40)	3.24 (0.15)	.05	.53
Occipital lobe (2 regions)				
Left lateral occipital	4.96 (3.80)	2.45 (0.14)	.03	.75
Right lateral occipital	5.38 (4.63)	2.52 (0.15)	.05	.53

* $p < .05$